Supporting Information

Tuning the aromatic backbone twist in dipyrrolonaphthyridinediones

Bartłomiej Sadowski,[a] Dominik Mierzwa,[a] Seongsoo Kang,[b] Marek Grzybowski,[a] Yevgen M. Poronik,[a] Andrzej L. Sobolewski,*[c] Dongho Kim*[b] and Daniel T. Gryko*[a]

[a] *Institute of Organic Chemistry, Polish Academy of Sciences, Kasprzaka 44/52, 01-224 Warsaw, Poland*

[b] *Department of Chemistry and Spectroscopy Laboratory for Functional π-Electronic Systems, Yonsei University, Seoul 03722, Korea*

[c] *Institute of Physics, Polish Academy of Sciences, Aleja Lotnikow 32/46, 02-668 Warsaw, Poland*

Table of contents

1. Experimental part

General Remarks. All reagents and solvents were purchased from commercial sources and were used as received unless otherwise noted. Reagent grade solvents (CH_2Cl_2, hexanes) were distilled prior to use. Toluene was dried by distillation over sodium and stored under argon. Transformations with moisture- and oxygen-sensitive compounds were performed under a stream of argon. The reaction progress was monitored by means of thin-layer chromatography (TLC), which was performed on aluminum foil plates, covered with silica gel 60 F254. Product purifications were done by means of column chromatography with Kieselgel 60. The identity and purity of prepared compounds were proved by ^1H NMR and ^{13}C NMR spectroscopies as well as by mass spectrometry (via EI-MS). HR-MS (EI): double-focusing magnetic sector instruments with EBE geometry were utilized. NMR spectra were measured on 500 MHz instrument. Chemical shifts (δ, ppm) were determined with $CDCl_3$ as the internal reference; J values are given in Hz. All melting points for crystalline products were measured with an automated melting point apparatus and are given without correction.

Improved synthesis of 1,4-di(pyrrol-1-yl)butane-1,4-dione (2)

To a solution of succinamide (9.87 g, 85.0 mmol) in acetic acid (300 mL) 2,5-dimethoxytetrahydrofuran (29 mL, 224 mmol) was added and the resulting mixture was stirred under reflux for 2.5 h. Acetic acid was evaporated in vacuo and the residue was basified with saturated sodium carbonate and extracted with dichloromethane/methanol 10/1 (4 times, methanol increases the solubility of the product). The combined organic layers were washed with water and dried over anhydrous sodium sulfate in the presence of ~5 g of activated carbon and ~20 g of silica

gel. The solids were removed by filtration through a pad of celite, which was washed with dichloromethane. The filtrates were concentrated in vacuo and recrystallized from toluene/ethanol (~1/5) to give the pure product (8.74 g), and the repeated recrystallization from the concentrated filtrates provided second and third fractions of the crystals (overall 2.27 g). In total 11.01 g (50.9 mmol, 60%) of 1,4-di(pyrrol-1-yl)butane-1,4-dione (**2**) was obtained as a white crystalline solid.

^{1}H NMR (400 MHz, CDCl$_3$) δ 7.36 (br s, 4H, pyrrole: 2-H and 5-H), 6.36 – 6.26 (m, 4H, pyrrole: 3-H and 4-H), 3.34 (s, 4H, CH$_2$CH$_2$) (Lit.[1] ^{1}H NMR (500 MHz, CDCl$_3$) δ 7.36 (br s, 4H), 6.36 – 6.27 (m, 4H), 3.34 (s, 4H).
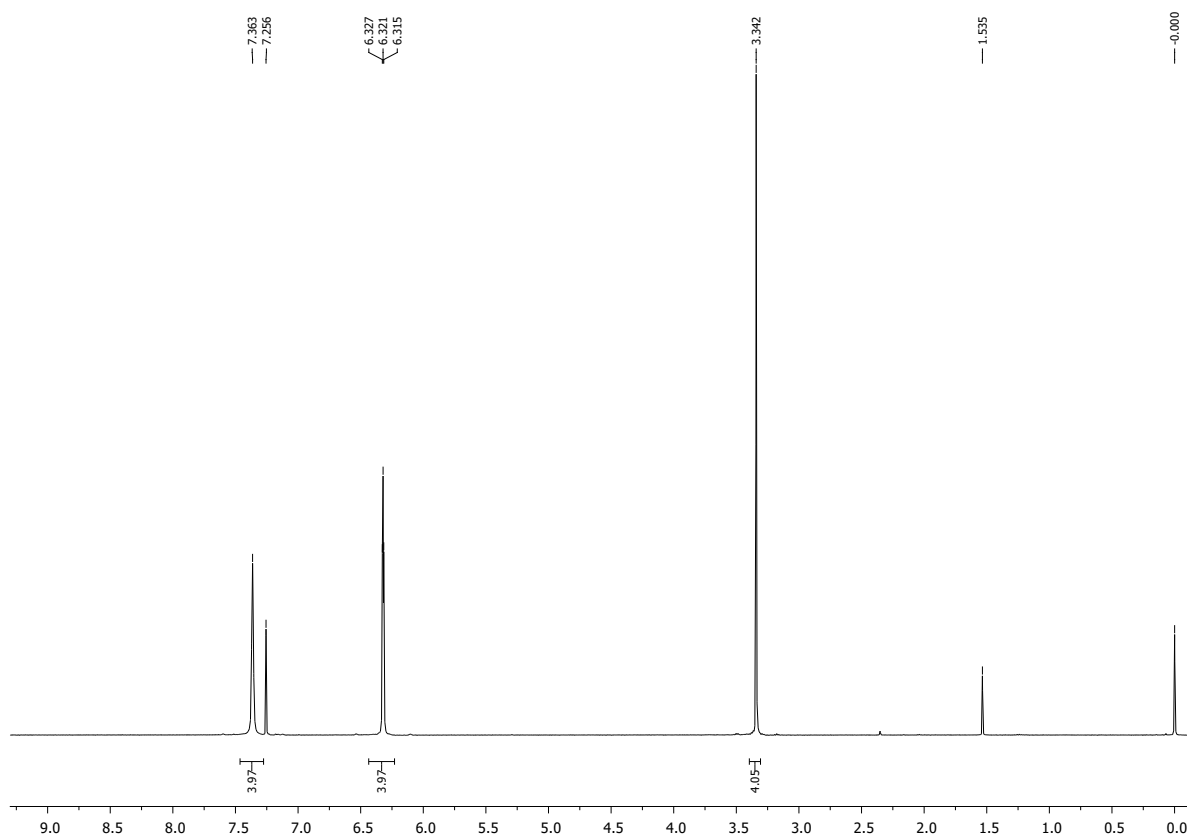

General procedure for the synthesis of DPNDphanes and analytical data for all new compounds.

Dipyrroyl derivative **2** (216.0 mg, 1.0 mmol), dicarboxylic acid (3.0 mmol) and 12 ml of CH$_2$Cl$_2$ were placed in a 50 mL round-bottom flask equipped with a magnetic stirring bar. Then,

trifluoroacetic anhydride (1.68 ml, 12 mmol) followed by trifiluoroacetic acid (0.64 ml, 6 mmol) were added. The mixture was stirred at room temperature for 3 hours. The reaction mixture was then poured into a beaker containing 50 ml of saturated aqueous $NaHCO_3$ and mixed (CO_2 gas evolved). When the evolution of carbon dioxide was no longer observed, layers were separated. Aqueous layer was extracted three times with dichloromethane, and the combined organic layers were washed with water and dried over Na_2SO_4. The title compounds were separated using column chromatography (SiO_2, dichloromethane : hexanes 3:1).
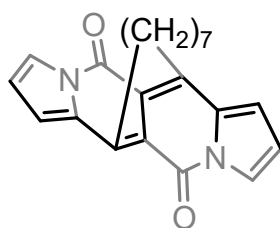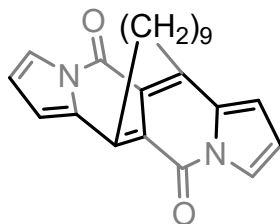

1(6,12)-Dipyrrolo[1,2-*b*:1',2'-*g*][2,6]naphthyridinacyclooctaphane-5,11-dione **(4).** Prepared using nonanedioic acid (565.1 mg, 3.0 mmol). Product **4** was obtained as a dark red solid (11.0 mg, 3% yield). Mp. 219-221°C. ^{1}H NMR (500 MHz, CDCl$_3$) δ 7.74 (d, J_1 = 3.5 Hz, J_2 = 1.5 Hz, 2H), 6.78 (d, J_1 = 3.5 Hz, J_2 = 1.0 Hz, 2H), 6.52 (t, 2H, J = 3.3 Hz), 4.05-3.99 (m, 2H), 2.87-2.82 (m, 2H), 1.57-1.47 (m, 4H), 0.93 (br s, 2H), 0.78 (br s, 2H), 0.45 (br s, 2H). ^{13}C NMR (151 MHz, CDCl$_3$) δ 160.1, 142.7, 134.6, 123.7, 121.1, 116.4, 115.9, 33.7, 29.1, 28.1, 26.5. HR-MS (EI): calcd for $C_{21}H_{20}N_2O_2$: 332.1525; found: 332.1523.
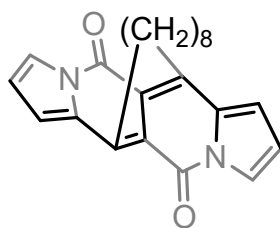
1(6,12)-Dipyrrolo[1,2-*b*:1',2'-*g*][2,6]naphthyridinacyclononaphane-5,11-dione **(5).** Prepared using decanedioic acid (606.0 mg, 3.0 mmol). Product **5** was obtained as a red solid (52.1 mg, 15% yield). Mp. 240-243°C. ^{1}H NMR (500 MHz, CDCl$_3$) δ 7.77 (dd, J_1 = 3.0 Hz, J_2 = 1.5 Hz, 2H), 6.84 (dd, J_1 = 3.5 Hz, J_2 = 1.5 Hz, 2H), 6.52 (t, J = 3.3 Hz, 2H), 4.30-4.25 (m, 2H), 2.89-2.84 (m, 2H),

1.89-1.83 (m, 2H), 1.62-1.48 (m, 4H), 1.07-0.98 (m, 2H), 0.71-0.63 (m, 2H), 0.16-0.08 (m, 2H). ^{13}C

NMR (151 MHz, CDCl$_3$) δ 160.1, 145.3, 133.4, 121.6, 121.2, 116.2, 115.7, 30.8, 29.9, 29.8, 28.8.

HR-MS (EI): calcd for C$_{22}$H$_{22}$N$_2$O$_2$: 346.1681; found: 346.1688.

1(6,12)-Dipyrrolo[1,2-*b*:1',2'-*g*][2,6]naphthyridinacyclodecaphane-5,11-dione **(6).** Prepared

using undecanoic acid (649.3 mg, 3.0 mmol). Product **6** was obtained as a red solid (12 mg, 3%

yield). Mp. 197-199°C. ^{1}H NMR (500 MHz, CDCl$_3$) δ 7.78 (dd, J_1 = 3.0, J_2 = 1.0 Hz, 2H), 6.84 (dd,

J_1 = 4.0 Hz, J_2 = 1.5 Hz, 2H), 6.52 (t, J = 3.5 Hz, 2H), 4.46-4.40 (m, 2H), 2.88-2.83 (m, 2H), 2.03-

1.99 (m, 2H), 1.45-1.30 (m, 4H), 0.87-0.78 (m, 4H), 0.77-0.61 (m, 4H). ^{13}C NMR (151 MHz,

CDCl$_3$) δ 160.1, 144.1, 133.1, 121.8, 119.7, 116.5, 115.7, 29.5, 29.2, 28.5, 27.1, 26.0. HR-MS (EI):

calcd for C$_{23}$H$_{24}$N$_2$O$_2$: 360.1838; found: 360.1835.

2. X-ray data

Crystal packing:

van der Waals interactions

2.410 Å   2.486 Å

complementary C–H•••O interactions within column

packing in column

2.606 Å

2.606 Å

complementary C–H•••O interactions between columns
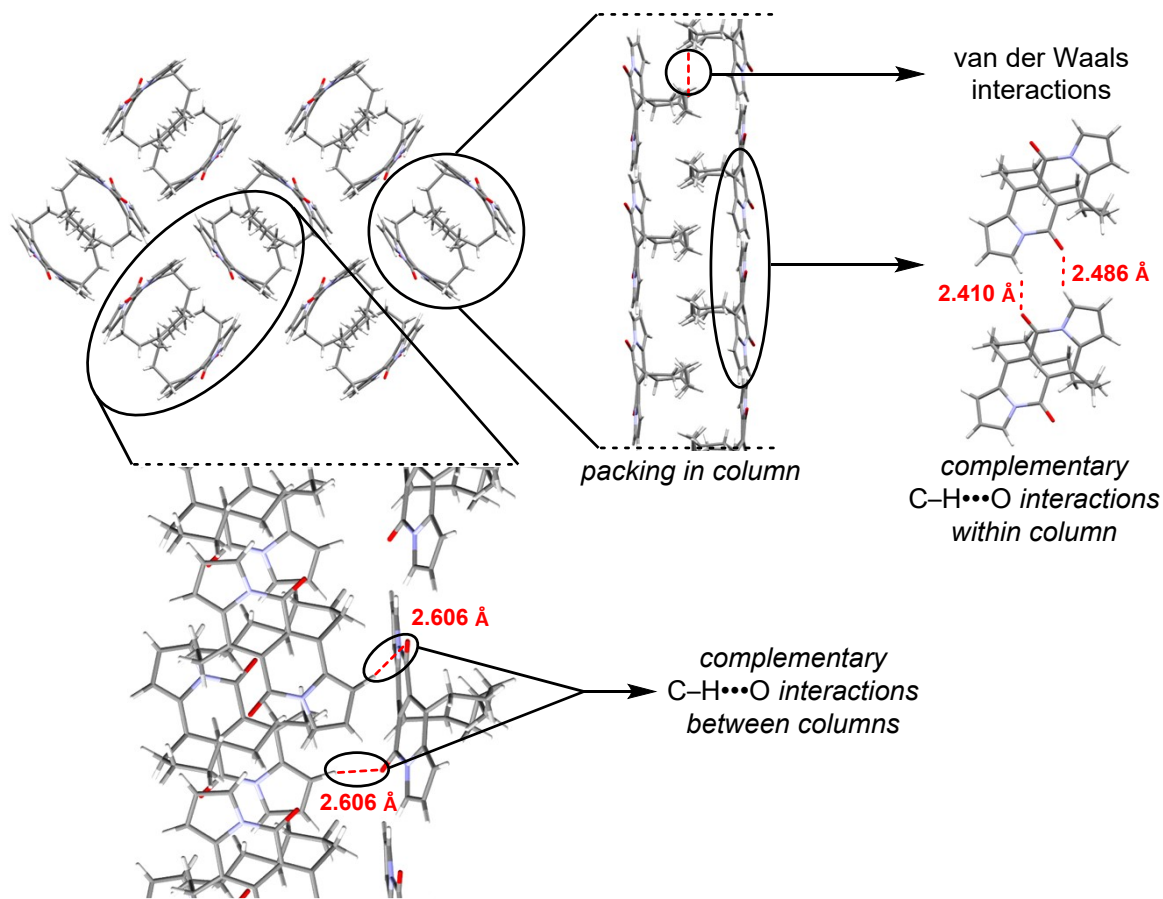
Table S1. Summary of crystal data for derivative **5**.

Compound	**5**
CCDC	2125168
Chemical formula	$C_{22}H_{22}N_2O_2$
Crystal system	Monoclinic
Space group	P 21/c
a (Å)	9.14752(2)
b (Å)	13.0433(4)
c (Å)	14.6294(4)
α (°)	90
β (°)	102.573(2)
γ (°)	90
Volume (Å³)	1764.66(8)
Z	4

Density (Mg m^{-3})	1.304
Temperature (K)	296
F(000)	736.0
Indep. Refl.	2465
Final R indices [I > 2σ(I)]	R = 0.0613 R$_w$ = 0.1801
S	1.100

3. Spectroscopic measurements

Steady-state measurement

Steady-state absorption spectra were measured on a UV/Vis spectrometer (Varian, Cary5000) and photoluminescence spectra were measured on a fluorescence spectrophotometer (Hitachi, F-2500). Photoluminescence spectra are spectrally corrected by using correction factor of the fluorescence spectrophotometer. Anhydrous-grade solvents were purchased from Sigma-Aldrich and used without further purification. All steady-state measurements carried out by using a quartz cuvette with a pathlength of 1 cm at ambient temperatures.

Femtosecond Transient Absorption and Transient Absorption Anisotropy.

Dual-beam femtosecond time-resolved transient absorption (TA) spectrometer consisted of two independently-tunable home-made noncollinear optical parametric amplifiers (NOPA) pumped by a regeneratively amplified Ti:sapphire laser system (Spectra-Physics, Hurricane-X) operating at 3 kHz repetition rate and an optical detection system. The NOPA was based on non-collinearly phase-matching geometry, which was easily color-tuned by controlling optical delay between white light continuum seed pulses (450-1400 nm) and visible pump pulses (400 nm) produced by using a sapphire window and BBO crystal, respectively. The generated visible OPA pulses had a pulse width of ~ 35 fs and an average power of 10 mW at 3 kHz repetition rate in the range 500-700 nm after a fused-silica prism compressor. Two OPA pulses were used as the pump and probe pulses, respectively, for TA measurement. The probe beam was split into two parts. The one part of the probe beam was overlapped with the pump beam at the sample to monitor the transient (signal), while the other part of the probe beam was passed through the sample without overlapping the

pump beam to compensate the fluctuation of probe beam. The time delay between pump and probe beams was carefully controlled by making the pump beam travel along a variable optical delay (Newport, ILS250). To obtain the time-resolved transient absorption difference signal at specific wavelength, the monitoring wavelength was selected by using a narrow interference filter (FWHM ~10 nm). By chopping the pump pulses at 47 Hz, the modulated probe pulses as well as the reference pulses were detected by two separate photodiodes (New Focus, Femtowatt Photoreceiver). The modulated signals of the probe pulses were measured by a gated-integrator (SRS, SR250) and a lock-in amplifier (EG&G, DSP7265) and stored in a personal computer for further signal processing. In general, experimental conditions, time-resolutions of less than 50 fs were achieved. For transient absorption anisotropy (TAA) measurement, both $I_{//}(t)$ and $I_{\perp}(t)$ signals were collected simultaneously by combination of polarizing beam-splitter cube and dual lock-in amplifiers as following equation:[1]

$$r(t) = [\ I_{//}(t) - I_{\perp}(t)]\ /\ [\ I_{//} + 2I_{\perp}(t)]$$

where $I_{//}(t)$ and $I_{\perp}(t)$ represent TA signals with the polarization of the pump and probe pulses being mutually parallel and perpendicular, respectively. The pump pulses were set to vertical polarization and that of probe pulse was set to 45˚ with respect to the pump pulse by using Glan-laser polarizers and half-wave plates. After the probe pulse passes through the sample cell, it was split by polarizing beam-splitter cube and then detected by two separate photodiodes. Two gated-integrators and two lock-in amplifiers record the signal simultaneously within a single scan. As a standard anisotropy measurement showed a clean single exponential decay with reorientational relaxation times of 122.1 ± 0.3 ps and the initial anisotropy r_0 value of 0.39 ± 0.02 for rhodamine 6G dye in methanol, which are well-matched with other references. For all TAA measurements, a thin absorption cell with a path length of 0.5 mm was used to eliminate additional chirping.

Picosecond time-resolved fluorescence measurements.

---

[1] C. K. Min, T. Joo, M. C. Yoon, C. M. Kim, Y. N. Hwang, D. Kim, N. Aratani, N. Yoshida, A. Osuka, *J. Chem. Phys*., **2001**, 114, 6750-6758.

A time-correlated single-photon-counting (TCSPC) system was used for measurements of spontaneous fluorescence decay. As an excitation light source, we used a mode-locked Ti:sapphire laser (Spectra Physics, MaiTai BB) which provides ultrashort pulse (center wavelength of 800 nm with 80 fs at FWHM) with high repetition rate (80 MHz). This high repetition rate was reduced to 800 kHz by using homemade pulse-picker. The pulse-picked output was frequency doubled by a 1-mm-thick BBO crystal (type-I, θ = 29.2°, EKSMA). The fluorescence was collected by a microchannel plate photomultiplier (MCP-PMT, Hamamatsu, R3809U-51) with a thermoelectric cooler (Hamamatsu, C4878) connected to a TCSPC board (Becker & Hickel SPC-130). The overall instrumental response function was about 25 ps (FWHM). A vertically polarized pump pulse by a Glan-laser polarizer was irradiated to samples, and a sheet polarizer set at an angle complementary to the magic angle (54.7°), was placed in the fluorescence collection path to obtain polarization-independent fluorescence decays.
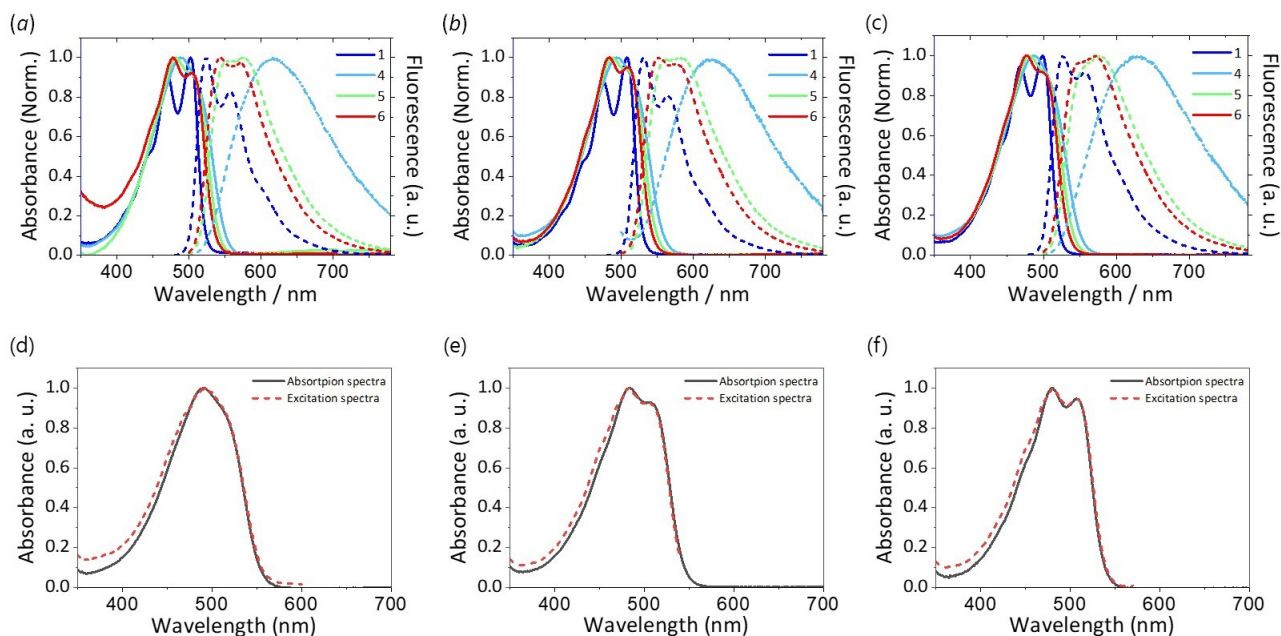
Figure S1. Absorption and normalized emission spectra (excited at 470 nm) of DPNDphanes in (a) THF, (b) C_6H_5CN and (c) MeCN. Absorption and excitation spectra (excitation spectra obtained by the maximum positions of the emission spectra of all species) for compounds (d) **4**, (e) **5** and (f) **6**.

Figure S2. The time-resolved fluorescence decay profiles in DPNDphanes in toluene (upper) and

Figure S3. Femtosecond transient absorption spectra and decay time profiles of **1** in toluene.

MeCN (lower) obtained by the time-correlated single photon counting (TCSPC) spectroscopy.

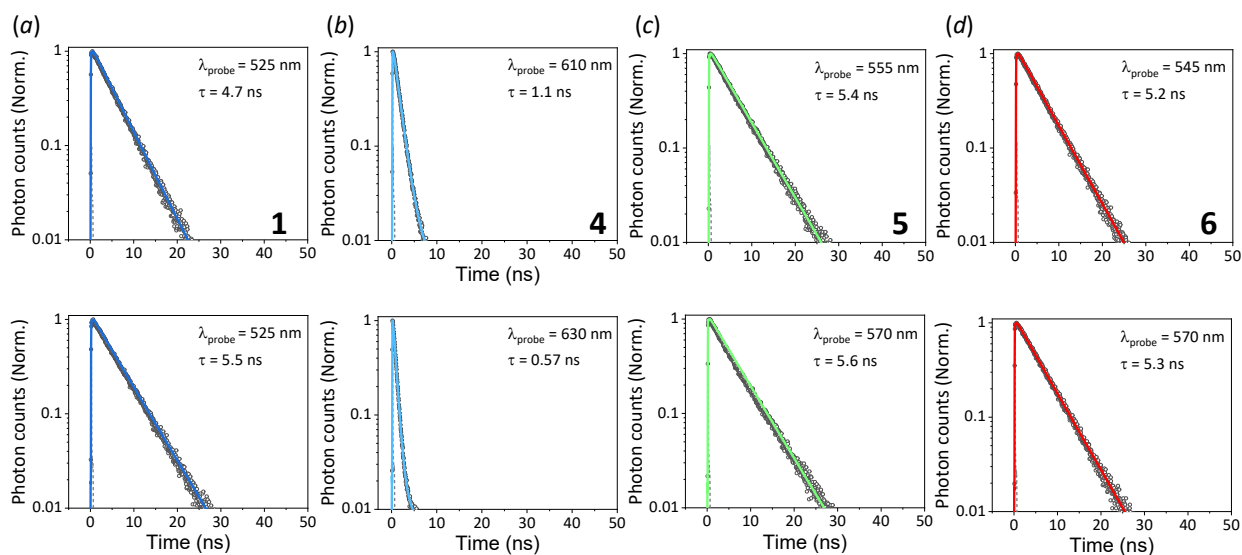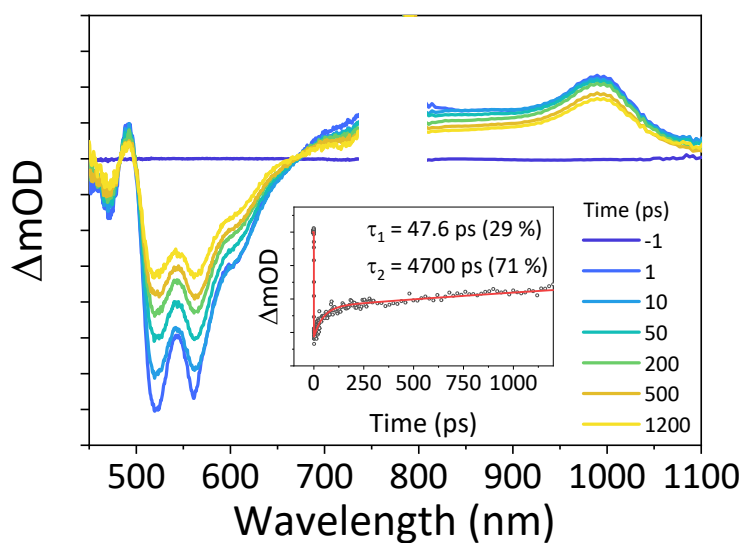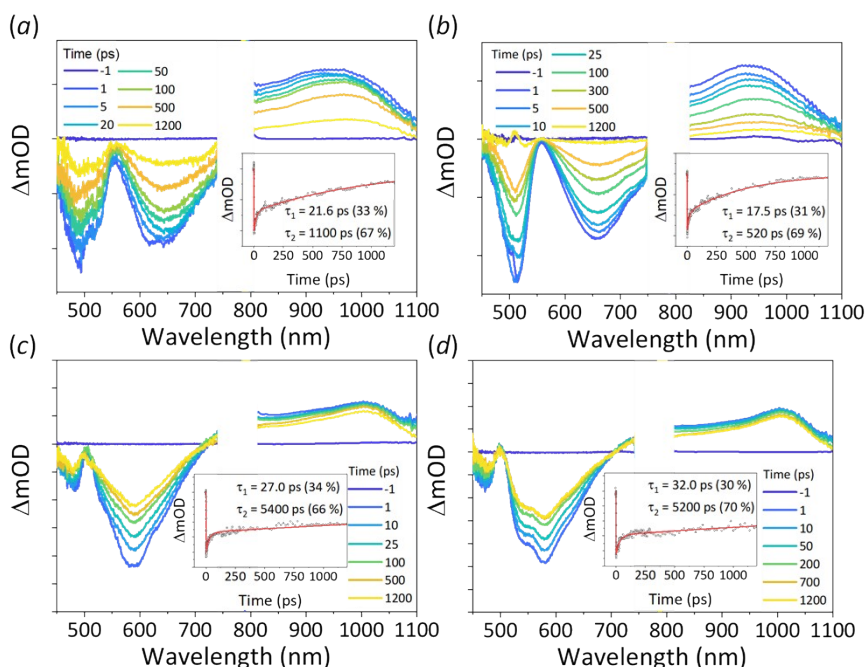**Figure S4.** Femtosecond transient absorption spectra and decay time profiles of (a) **4** in toluene, (b) **4** in MeCN, (c) **5** in toluene, and (d) **6** in toluene.

4. Computational details

General Remarks. The ground-state equilibrium geometries of considered molecular systems were determined with the second-order Møller-Plesset (MP2) *ab initio* method.[2] Vertical electronic excitation energies and equilibrium geometries of lowest singlet excited states were determined employing the second-order algebraic-diagrammatic-construction (ADC(2)) method[3] and with the simplified second-order coupled-cluster (CC2) method.[4] The analysis of the electronic wave functions of the excited states were performed in the natural transition orbitals (NTO) representation.[5] In all calculations the correlation-consistent polarized valence-split double-ζ basis set (cc-pVDZ)[6] was employed. Calculations were performed with the TURBOMOLE 7.3 program package[7] making use of the resolution-of-the-identity (RI) approximation. Additionally, in order to check dependence of determined quantities on theoretical method, these calculations were also performed with the aid of a simplified second-order coupled-cluster (CC2) method.[3]

[2] C. Møller, M. S. Plesset, *Phys. Rev.* **1934**, *46*, 618-622.

[3] J. Schirmer, *Phys. Rev. A: At., Mol., Opt. Phys.* **1982**, *26*, 2395-2416.

[4] O. Christiansen, H. Koch, P. Jørgensen, *Chem. Phys. Lett.* **1995**, *243*, 409-418.

[5] R. L. Martin, *J. Chem. Phys.* **2003**, *118*, 4775-4777.

[6] T.H. Dunning, *J. Chem. Phys.* **1989**, *90*, 1007-1023.

[7] TURBOMOLE V7.3 2018, a development of University of Karlsruhe and Forschungszentrum Karlsruhe GmbH, 1989–2007, TURBOMOLE GmbH, since 2007; available from http://www.turbomole.com.

The DFT calculations were performed with the three-parameter Becke, Lee, Yang, Parr exchange-correlation functional (B3LYP)[8] with dispersion correction (D3) of Grimme.[9]

Table S2. Average deviation from planarity (ϕ) for DPND derivatives **4^open** and **4-6**. Optimization of the molecular geometry in the ground electronic state (S_0) was performed with MP2/cc-pVDZ, while for the excited electronic state either ADC(2)/cc-pVDZ or CC2/cc-pVDZ method was used without symmetry constraints.

Compound/State	S_0	S_1	
		ADC(2)	CC2
4^open	7.4°	5.6°	6.0°
4	32.8°	43.6°	45.5°
5	27.8°	25.6°	26.0°
6	15.4°	12.8°	-[a]

[a] The CC2 geometry optimization of the S_1 state for compound **6** was not possible due to large size of the molecule.

Table S3. Vertical fluorescence energy from the lowest excited singlet state (ΔE), oscillator strength (f), and dipole moment (μ), determined with the ADC(2)/cc-pVDZ method. Results obtained with the C_2 symmetry constrains are given in parentheses.

Compound	ΔE/eV	f	μ (S_1)/ μ (S_0) / Debye
4^open	2.37	0.63	0.20/0.19
4	0.20 (1.99)	0.0 (0.46)	6.50(2.09)/6.69(2.37)
5	2.19 (1.99)	0.50 (0.47)	1.92(1.87)/2.07(2.16)
6	2.16 (2.21)	0.50 (0.52)	2.47(1.51)/1.49(1.70)

Table S4. Vertical fluorescence energy from the lowest excited singlet state (ΔE), oscillator strength (f), and dipole moment (μ), determined with the CC2/cc-pVDZ method. Results at the C_2 symmetry in parentheses.

Compound	ΔE/eV	f	μ (S_1)/ μ (S_0) / Debye
4^open	2.52	0.54	1.59/0.27
4	1.30 (2.22)	0.09 (0.42)	4.20(1.82)/3.01(1.93)
5	2.35 (2.23)	0.45 (0.43)	1.64(1.76)/1.64(1.59)

[8] a) A. D. Becke, *J. Chem. Phys.* **1993**, *98*, 5648-5652; b) C. Lee, W. Yang, R. G. Parr, *Phys. Rev. B: Condens. Matter Mater. Phys.* **1988**, *37*, 785-789.
[9] S. Grimme, *J. Comput. Chem.* **2006**, *27*, 1787-1799.

Table S5. Vertical absorption energy (ΔE), oscillator strength (f), and dipole moment (μ) of the lowest excited states of a given symmetry (within the Cs point group) computed with the aid of the ADC(2)/cc-pVDZ method at the MP2-optimized geometry of the ground state.

1				4			
State	ΔE/eV	f	μ/D	State	ΔE/eV	f	μ/D
S_0	0.0	-	0.50	S_0	0.0	-	2.86
T_1	1.68	-	0.50	T_1	1.55	-	2.72
S_1	2.79	0.612	0.52	T_2	2.61	-	2.76
T_2	2.85	-	0.61	S_1	2.66	0.476	2.96

5				6			
State	ΔE/eV	f	μ/D	State	ΔE/eV	f	μ/D
S_0	0.0	-	2.22	S_0	0.0	-	1.45
T_1	1.56	-	2.14	T_1	1.59	-	1.37
S_1	2.63	0.492	2.17	S_1	2.66	0.528	1.36
T_2	2.76	-	2.12	T_2	2.78	-	1.42

Calculations of strain energies for dyes 4-6:
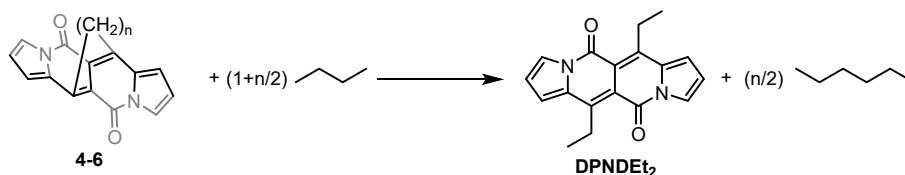
	Final heat of formation / Hartree	
System	D3-DFT/B3LYP/cc-pVDZ	MP2/cc-pVDZ
4	-1071.6849277440	-1069.0403037529
5	-1110.9888209440	-1108.2491419521
6	-1150.2861779170	-1147.4384419958
DPNDEt$_2$	-955.0550471230	-952.7237918176
***n*-butane**	-158.3421904554	-157.8988226344
***n*-hexane**	-236.9183596297	-236.2602779707
	Strain energies in Hartree/kcal·mol^{-1}	
ΔH(n=7)	0.044521034/27.9	0.049759107/31.2
ΔH(n=8)	0.028712421/18.0	0.021650528/13.6
ΔH(n=9)	0.019440035/12.2	0.013078197/8.2

5.   Cyclic voltammetry (CV)

The electrochemical properties of compounds **1**, **4-6** were investigated by cyclic voltammetry. All the tested compounds exhibit irreversible oxidation processes around 1.28–1.32 V. On the other hand, compounds **1**, **5**, **6** show well resolved reversible reduction wave at potentials around -0.92-

1.14 V, only compound **4** displays a quasi-reversible reduction wave at -1.09 V (*vs*. Ag/AgCl/NaCl) (Table SX, Figure SX). The redox characteristics for compounds **5** and **6** are in good agreement with those for non-bridged DPND **1**, contrariwise **4** which shows complex oxidation processes. The latter occur the most probably due to a more strained molecular geometry with a shorter bridge.

Table S6. Redox potentials (vs. Ag/AgCl/NaCl) of compounds **1**, **4**, **5** and **6**[a]

Cmpd	E_{ox}^{PA} / V	E_{ox}^{onset} / V	IP / eV	E_{red}^{PA} / V	E_{red}^{PC} / V	$E_{red}^{1/2}$ / V	E_{red}^{onset} / V	EA / eV
1	1.28	1.15	5.49	--0.92	−1.10	−1.01	−0.96	−3.38
4	1.25	1.13	5.47		−1.09		−0.98	−3.36
5	1.32	1.19	5.53	−0.99	−1.08	−1.03	−0.98	−3.36
6	1.32	1.19	5.53	−1.03	−1.14	−1.08	−1.02	−3.32

[a] – Measurements conditions: electrolyte (NBu$_4$ClO$_4$, c = 0.1 M); solvent: dry, degassed dichloromethane; potential sweep rate: 100 mV/s; working electrode: GC; auxiliary electrode: Pt wire; reference electrode: Ag/AgCl/NaCl(satd); all measurements were carried out at room temperature and under Ar atmosphere.

A: B: C: D:
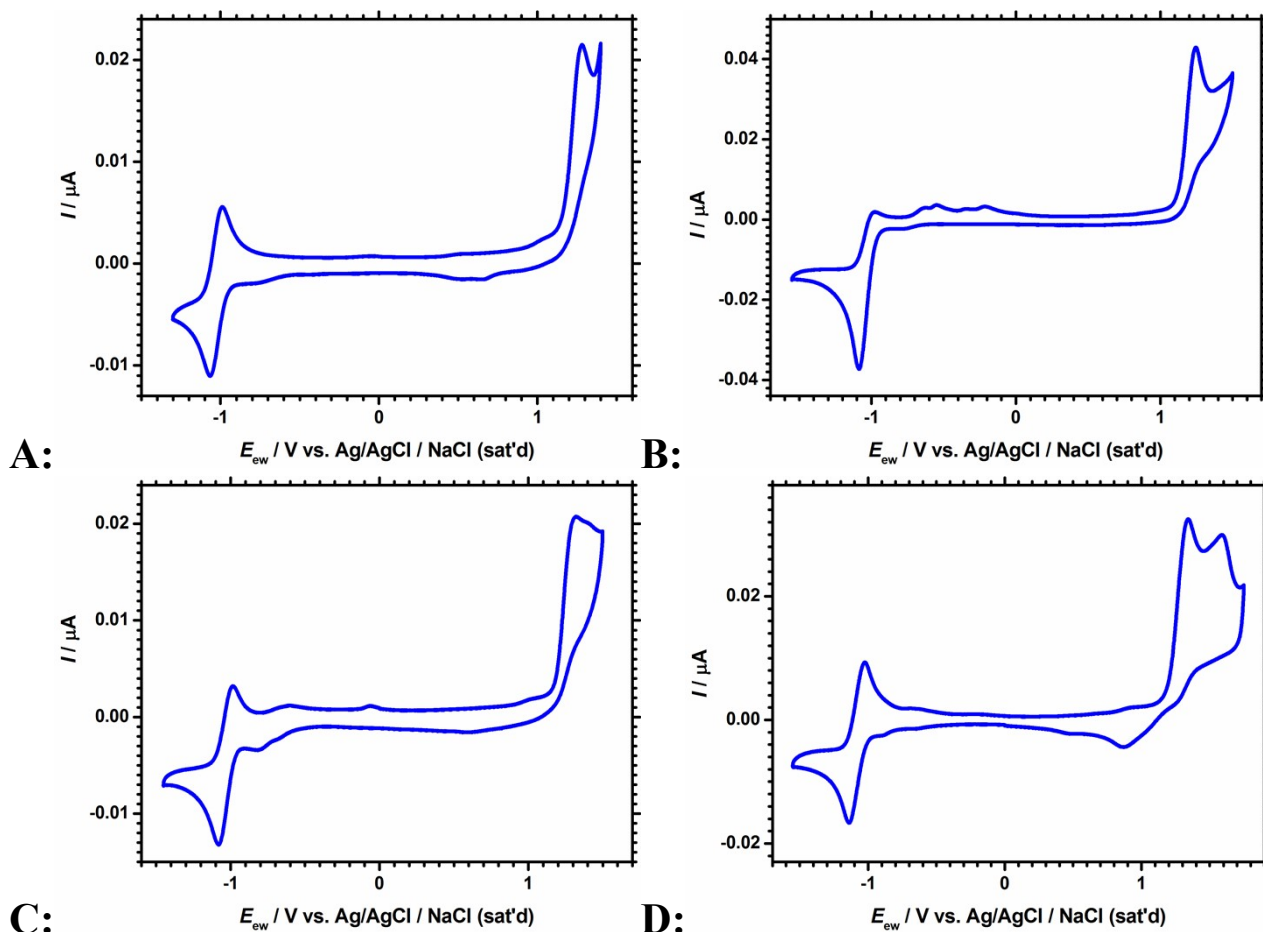
Fig. S5. Cyclic voltammograms of A: **1**, B: **4**, C: **5**, D: **6** in CH$_2$Cl$_2$.

6. ^{1}H and ^{13}C NMR spectra of compounds 4-6.

Note: despite the fact that the samples were dried overnight under high vacuum at 70 °C there are traces of solvents that disturb an alkyl region of NMR spectra.

4
(500 MHz, CDCl₃)

$^{13}C\{^1H\}$ NMR
(151 MHz, CDCl₃)

5
(500 MHz, CDCl₃)

5
¹³C{¹H} NMR
(151 MHz, CDCl₃)

S16

^{1}H NMR
6
(500 MHz, CDCl$_3$)

7.780
7.778
7.774
7.771
7.260 CDCl3
6.843
6.840
6.835
6.833
6.532
6.525
6.518

4.462
4.453
4.439
4.436
4.429
4.427
4.413
4.403

2.878
2.869
2.860
2.852
2.843
2.834

2.032
2.014
2.005
1.987

1.390
1.371
1.349
1.333
1.326
1.305
0.866
0.829
0.821
0.799
0.790
0.782
0.772
0.726
0.714
0.703
0.681
0.660
0.636
0.624

1.96
2.01
2.00
2.06
2.04
2.05
4.18
4.20
4.24

f1 (ppm)

^{13}C{^{1}H} NMR
6
(151 MHz, CDCl$_3$)

160.139
144.142
133.061
121.771
119.669
116.519
115.692
77.160 CDCl3
29.495
29.198
28.548
27.116
26.025

f1 (ppm)

S17